Int. J. Heat Mass Transfer. Vol. 29, No. 3, pp. 391–402, 1986
Printed in Great Britain

0017–9310/86 $3.00 + 0.00

Mixed laminar convection in a horizontal tube with natural convection around its boundaries

J. PASCAL COUTIER* and RALPH GREIF†

* Passive Research and Development, Lawrence Berkeley Laboratory, Berkeley, CA 94720, U.S.A.
† Mechanical Engineering Department, University of California, Berkeley, CA 94720, U.S.A.

(*Received* 25 *April* 1985 *and in final form* 19 *September* 1985)

Abstract—The laminar flow and heat transfer within a horizontal tube surrounded by a liquid medium are studied both experimentally and numerically. Emphasis is given to flow regimes where a buoyant effect on the forced flow is exhibited inside the tube. The outer surface of the tube is also subjected to natural convection resulting from the temperature difference between the wall and the surrounding fluid. Detailed analyses are performed for a number of cases with various fluids, inlet temperatures and fluid flows. It is found that the variable wall temperature has a marked effect on the secondary flow patterns within the tube as well as on the heat transfer.

INTRODUCTION

THIS PAPER describes a study of fluid flow and heat transfer inside a horizontal circular tube immersed in a liquid medium. The hot fluid within the tube exchanges its energy with the surrounding liquid through the tube wall around which natural convection occurs. The problem of convection within a tube including the interaction of a convecting external fluid is often referred to as the 'conjugate problem'. The present study is further complicated by the presence of strong buoyant forces in the internal fluid motion. These combined effects produce significant angular variations of the wall temperature, making the problem three-dimensional. The understanding of the phenomena described above is essential for predicting accurately the laminar heat transfer in tubes immersed in liquids.

Several authors have addressed the question of the natural convective flow around a cylinder. However, only a few studies have been carried out on the conjugate problem, especially when natural convection is important within and outside the tube. Kuehn and Balvanz [1] studied numerically the problem of conjugate heat transfer for forced turbulent convection inside a tube with laminar external convection. Sunden [2] modeled the conjugate heat transfer from a circular cylinder with a heated solid core region. Faghri and Sparrow [3] studied the laminar forced convective heat transfer in a horizontal pipe for boundary conditions involving natural convection and radiation to an infinite fluid; they found that the overall pipe Nusselt number was essentially insensitive to the variation of the outside heat transfer coefficient, and that both the wall and fluid temperature profiles were individually more responsive to variable external conditions. However, their study did not account for the angular variation of the external film coefficient. Abdelmeguil and Spalding [4] studied the turbulent flow in pipes where buoyant forces are important. They solved the problem numerically for vertical, horizontal and tilted pipes. Relevant work on pipe flows is also reported by Javeri [5] and Golos [6]. Natural convection around a cylinder was treated by Kuehn and Goldstein [7, 8], Churchill and Usagi [9], Peterka and Richardson [10] and Mojtabi and Caltagirone [11]. Studies emphasizing natural convection effects outside the tube wall are reported by Lin and Chao [12], Aihara and Saito [13], Acrivos [14], Gill and Bardhun [15], Churchill and Hsu [16] and Morgan [17].

The purpose of the present study is to develop, through experimental results and numerical calculations, a better understanding of the heat transfer and fluid flow inside the heat exchanger tube when external natural convection takes place at the outer surface of the tube wall. Particular attention is given to the effect of wall temperature variation on fluid flow patterns and heat transfer rate.

THE EXPERIMENTAL STUDY

The test facility shown in Fig. 1 is described in detail in ref. [22]. The main features of the system are:

1. Two solar collectors with a total glazing area of 3.47 m^2 with long strip heaters attached to the rear of the absorber plates.
2. A cylindrical storage tank, made of steel, 1.52 m long and 0.51 m in diameter, wrapped with a 0.1-m-thick layer of foam glass insulation.
3. Collector to tank piping made of 2.5-cm-ID silicone hose, insulated with a 1.8-cm-thick elastomeric foam.
4. A heat exchanger made of two copper tubes, each with an outside diameter of 2.54 cm, wall thickness of 0.3 cm and length of 1.52 m. The two tubes were placed 0.35 m apart, parallel to the tank axis. There

NOMENCLATURE

A aspect ratio
A' characteristic velocity, $[gr_o/(T-T_w)]^{1/2}$
a_{nb} diffusion and convection coefficient
c_p heat capacity at constant pressure [J kg^{-1} K^{-1}]
d heat exchanger inside tube diameter [m]
$\mathbf{F}$ body force vector
$\mathbf{g}$ acceleration vector
g acceleration due to gravity [m s^{-1}]
Gr Grashof number, $\beta g d^3(T-T_w)\rho^2/\mu^2$
Gz Graetz number, $Re\ Pr\ \pi\ d/4L$
h height above a datum [m]
L heat exchanger tube length [m]
m mass flowrate [kg s^{-1}]
Nu Nusselt number, $h'd/k$
$Nu(\phi, z)$ local Nusselt number, function of ϕ and z
$\overline{Nu}(z)$ average local Nusselt number, function of z
$\overline{Nu}$ average Nusselt number
p pressure [Pa]
p_o thermodynamic pressure [Pa]
P dimensionless pressure, $p/\rho v_m^2$
Pr Prandtl number, $c\mu/k$
r radial coordinate
r_o tube radius [m]
Ra inner flow Rayleigh number, $Pr\ \beta^2 g d^3(T_w-T)/\mu^2$
Re Reynolds number, $\rho v_m d/\mu$
S source term
T temperature [°C]
T_{in} inlet temperature [°C]
T_{out} outlet temperature [°C]
T_w wall temperature [°C]
$\mathbf{u}$ velocity vector
u radial component of the velocity
U dimensionless radial velocity
v circumferential component of the velocity
v_m mean axial velocity
v_s average cross-sectional velocity
V dimensionless circumferential velocity
W dimensionless axial velocity
z axial component
Z dimensionless axial coordinate.

Greek symbols

α thermal diffusivity [m^2 s^{-1}]
β coefficient of thermal expansion [K^{-1}]
Γ diffusion coefficient
ε dimensionless temperature gradient, $\beta(T-T_w)$
η dimensionless radial coordinate
θ dimensionless temperature, $(T-T_w)/(T_{in}-T_w)$
μ dynamic viscosity [Pa s]
μ_w dynamic viscosity at the wall [Pa s]
ν kinematic viscosity [m^2 s^{-1}]
ρ density [kg m]
ρ_w density at the wall (kg m)
ϕ angular coordinate
ψ any dependent variable in the code.

Subscripts

b bulk
in inlet
out outlet
o outside fluid
w wall.

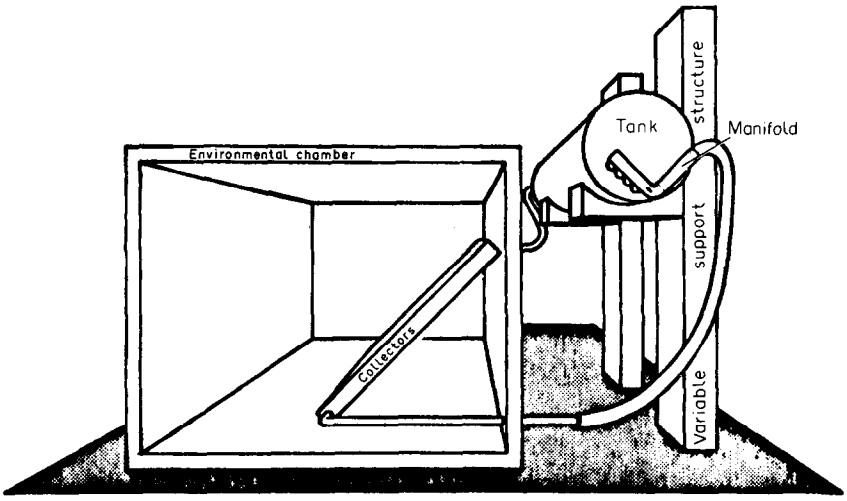

FIG. 1. Schematic of the test facility.

is a straight 0.3-m-long section prior to the entrance of the copper test section. This portion of the tube, located outside of the storage tank, has the same diameter as the test section.

The loop was comprised of the collectors, the piping and the heat exchanger tube. The fluid was circulated through the loop by a small 1/8 h.p. pump. The heat exchanger loop contained about 18 dm^3 of fluid, which was either water or a solution (60% by weight) of propylene glycol. The storage tank had a capacity of 300 dm^3 of water.

Twenty-four copper–constantan thermocouples were located at three equally spaced axial locations within the storage tank to permit a detailed evaluation of the water temperature surrounding the heat exchanger tube. The thermocouples, made by Omega Engineering, were 2 mm in diameter and the outputs were calibrated to 0.05°C in a constant temperature bath. Four axial locations were chosen along the tube ($L/12$, $L/6$, $L/2$, $5L/6$) to record the internal fluid and wall temperatures (cf. Fig. 2). The last three locations coincided with the tank temperature grids, and the first location was added to provide additional information on the thermal boundary layer.

For most of the experiments, the internal thermocouples were located on the tube center line. At each of the four axial locations where the tube temperature was measured, five probes were used. Two of them recorded the fluid temperatures at the tube centre line and at two-thirds of the radius at an angle ϕ equal to 0° (cf. Fig. 3). Three wall temperatures were also measured. They were located on the north, east and south sides of the wall (when facing downstream), whereas the fluid temperature probes were inserted through a sealed hole on the west side of one of the tubes as shown in Fig. 3. The 'infinite' temperature was taken far above the tubes, where the water temperature was found experimentally to be uniform, but it changed with time as the heat transferred from the tubes warmed up the surrounding fluid. The maximum rate of change of the water temperature in the storage tank was 2°C h^{-1}. The results presented hereafter were based upon instantaneous measurements and were independent of time.

Table 1 summarizes the conditions used in each test. The Grashof and Rayleigh numbers shown in Table 1 are calculated using an average wall temperature defined as follows: $T_w = [T_w(z=0)+T_w(z=L)]/2$, where both inlet and outlet temperatures are the average values calculated over all angles.

THE NUMERICAL MODEL

The presence of the secondary flow requires that a three-dimensional analysis be carried out. The presence of buoyant forces means that the momentum and the energy equations must be solved simultaneously.

In this study, the following assumptions have been made:

1. steady-state conditions;
2. laminar flow;
3. incompressible fluid;
4. negligible viscous dissipation; and
5. constant physical properties, except for the density.

The Boussinesq approximation was used, which specifies the density to be a constant everywhere except in the body force term of the momentum equation, where it is assumed to vary linearly with temperature.

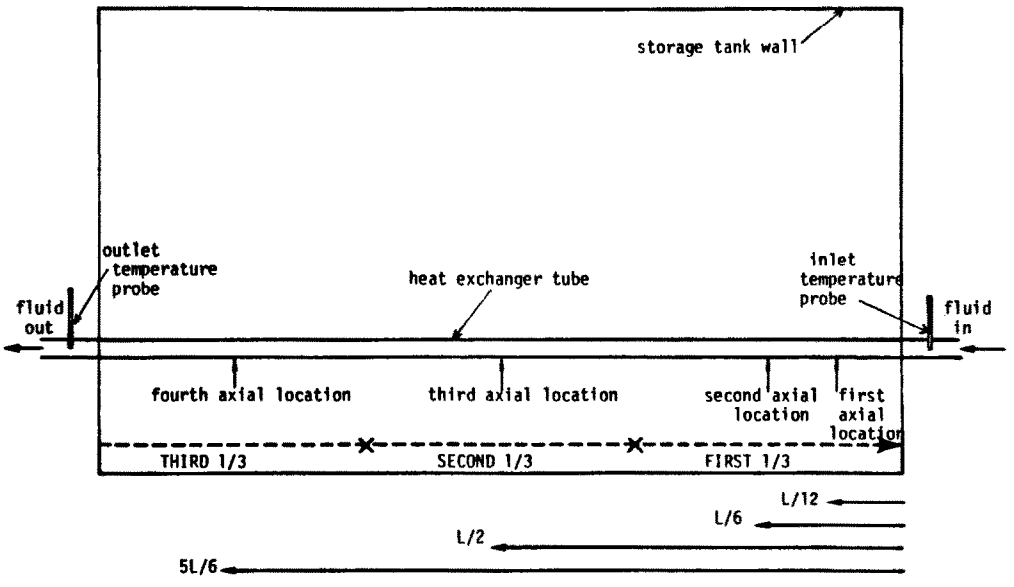

FIG. 2. Schematic of the heat exchanger tube.

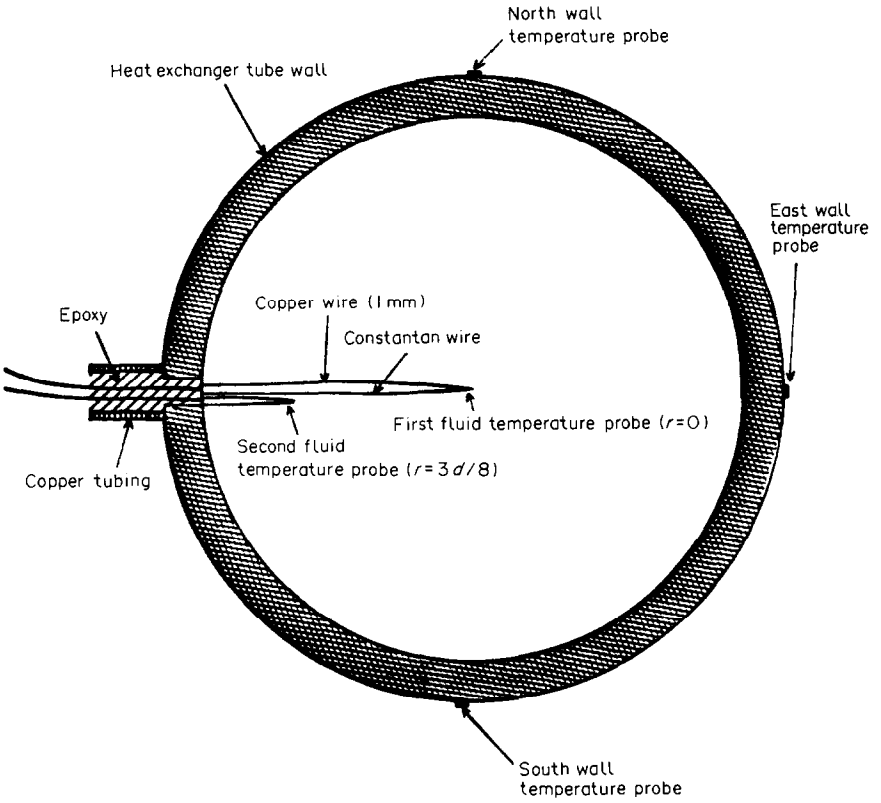

FIG. 3. Cross-section of the heat exchanger tube with locations of the temperature probes.

The following expression has been assumed for the density:

$$\rho = \rho_w[1-\beta(T-T_w)]. \tag{1}$$

A dimensionless form of the conservation equations can be written in cylindrical coordinates to yield:

conservation of mass

$$\frac{\partial U}{\partial \eta}+\frac{U}{\eta}+\frac{1}{\eta}\frac{\partial V}{\partial \phi}+\frac{\partial W}{\partial Z}=0 \tag{2}$$

conservation of momentum

r-direction

$$\frac{Gr}{Re^2}\left[U\frac{\partial U}{\partial \eta}+\frac{V}{\eta}\frac{\partial U}{\partial \phi}-\frac{V^2}{\eta}+W\frac{\partial U}{\partial Z}\right]$$
$$=-\frac{\partial P}{\partial \eta}-\frac{Gr}{Re^2}\theta\sin\phi+\frac{Gr}{Re^2(Gr)^{1/2}}$$
$$\times\left[\frac{\partial}{\partial \eta}\left(\frac{1}{\eta}\frac{\partial}{\partial \eta}(\eta U)\right)+\frac{1}{\eta^2}\frac{\partial^2 U}{\partial \phi^2}+\frac{\partial^2 U}{\partial Z^2}-\frac{2}{\eta^2}\frac{\partial V}{\partial \phi}\right] \tag{3}$$

ϕ-direction

$$\frac{Gr}{Re^2}\left[U\frac{\partial V}{\partial \eta}+\frac{V}{\eta}\frac{\partial V}{\partial \phi}+\frac{UV}{\eta}+W\frac{\partial V}{\partial Z}\right]$$
$$=-\frac{\partial P}{\eta\partial \phi}+\frac{Gr}{Re^2}\theta\cos\phi+\frac{Gr}{Re^2(Gr)^{1/2}}$$
$$\times\left[\frac{\partial}{\partial \eta}\left(\frac{1}{\eta}\frac{\partial}{\partial \eta}(\eta V)\right)+\frac{1}{\eta^2}\frac{\partial^2 V}{\partial \phi^2}+\frac{\partial^2 V}{\partial Z^2}+\frac{2}{\eta^2}\frac{\partial U}{\partial \phi}\right] \tag{4}$$

z-direction

$$U\frac{\partial W}{\partial \eta}+\frac{V}{\eta}\frac{\partial W}{\partial \Phi}$$
$$+W\frac{\partial W}{\partial Z}=-\frac{d}{L}\frac{\partial p}{\partial Z}\left(\frac{Gr}{Re^2}\right)^{-1/2}$$
$$+\frac{1}{Gr^{1/2}}\left[\frac{1}{\eta}\frac{\partial}{\partial \eta}\left(\eta\frac{\partial W}{\partial \eta}\right)+\frac{1}{\eta^2}\frac{\partial^2 W}{\partial \phi^2}+\frac{\partial^2 \theta}{\partial Z^2}\right] \tag{5}$$

conservation of energy

$$U\frac{\partial \theta}{\partial \eta}+\frac{V}{\eta}\frac{\partial \theta}{\partial \phi}+W\frac{\partial \theta}{\partial Z}=-\frac{1}{Pr(Gr)^{1/2}}$$
$$\times\left[\frac{1}{\eta}\frac{\partial}{\partial \eta}\left(\eta\frac{\partial \theta}{\partial \eta}\right)+\frac{1}{\eta^2}\frac{\partial^2 \theta}{\partial \phi^2}+\frac{\partial^2 \theta}{\partial Z^2}\right]. \tag{6}$$

Table 1. Summary of operating conditions for the five cases studied

Case No.	1	2	3	4	5
Fluid	Water	Water	Water	Glycol	Glycol
Flow-rate ($dm^3\ min^{-1}$)	0.282	1.130	0.512	0.659	1.059
Average axial velocity ($cm\ s^{-1}$)	0.616	2.466	1.118	1.438	2.310
Inlet temperature (°C)	68.5	37.9	61.6	46.7	50.0
Initial outer fluid temperature (°C)	27.6	15.0	32.3	32.8	24.9
Reynolds number	255	740	480	81	134
Rayleigh number (10^6)	1.9	1.25	2.0	1.3	2.2
Prandtl number	3.4	4.9	3.3	32.1	30.0
Gr/Re^2	9.0	0.46	2.6	9.2	4.1

The ratio Gr/Re^2 is a characteristic quantity for this problem. The cylindrical coordinate system was used, where ϕ is the angle around the pipe, r is the radial coordinate and z is the axial coordinate (cf. Fig. 4).

The boundary conditions for this problem are:

1. $u(r, \phi, z = 0) = v(r, \phi, z = 0) = 0$ (no secondary flow at the entrance to the heat exchanger tube)
2. $w(r, \phi, z = 0) = 2v_m/(1 - r^2/r_o^2)$
3. $T(r, \phi, z = 0) = T_{in} = \text{const.}$
4. $u(r = r_o, \phi, z) = v(r = r_o, \phi, z) = w(r = r_o, \phi, z) = 0$
5. $u(r = 0, \phi, z)$, $v(r = 0, \phi, z)$, $w(r = 0, \phi, z)$ and $T(r = 0, \phi, z)$ finite
6. symmetry about a vertical plane: for example, $u(r, \phi, z) = u(r, -\phi, z)$
7. the boundary condition at the wall was expressed as:

$$-kd\frac{\partial T}{\partial r} \quad (\text{at } r = d/2) = h_o d_o (T_{w_\phi} - T_{oo}) \qquad (7)$$

where T_{w_ϕ} is the angle-dependent wall temperature at a given axial location. The temperature drop across the highly conductive copper tube is neglected. The convective heat transfer coefficient h_o is calculated from the following correlation [17]:

$$Nu_o = 0.36 + 0.518 Ra_o^{0.25}/\Phi_1(Pr) \qquad (8)$$

where Ra_o is defined by:

$$Ra_o = Pr_o \rho_o^2 \beta_o g (T_{w_\phi} - T_{oo}) d_o^3/\mu_o^2 \qquad (9)$$

and $\Phi_1(Pr)$ by:

$$\Phi_1(Pr) = [1 + (0.559)/Pr)^{9/16}]^{4/9}. \qquad (10)$$

It is noted that T_{w_ϕ} is unknown *a priori* and varies both with ϕ and z. Its value is calculated from the numerical solution of the energy equation (6), subject to the boundary condition given in equation (7).

The program used to carry out the calculation was TOROID, a three-dimensional version of the program TEACH [18] adapted to cylindrical coordinates. The code solved the elliptic forms of the conservation equations in terms of a finite difference formulation as described by Humphrey [19]. The methodology used for solving the set of equations is described by Humphrey [19], Patankar, [20], Lavine [21] and in Appendix B of Coutier and Greif [22].

Calculations were carried out with $10 \times 16 \times 30$ (r, ϕ, z) and $15 \times 24 \times 45$ grids. Detailed comparisons were made for the velocity and temperature profiles and results showed excellent agreement for the two grids [23].

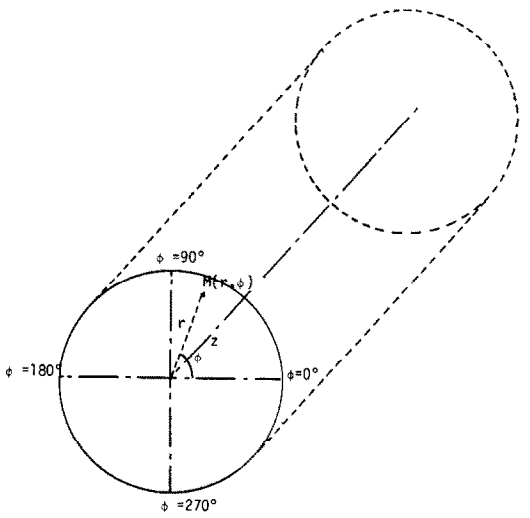

FIG. 4. Coordinate system.

RESULTS AND DISCUSSION

A. Temperature distribution

Five tests were analyzed in detail (cf. Table 1), which differed primarily in the magnitudes of the axial velocity and the inlet temperature. The axial variations of the measured and the calculated dimensionless temperatures are plotted in Figs. 5 and 6. All results are for the locations defined by $r = 0$ and $r = 3d/8$, $\phi = 0°$. The agreement between the experimental results and the theoretical predictions is good; the difference is less than 10% for all points except for the first two axial locations where the gradients are very large. It is noted that, near the inlet, the calculated temperatures for

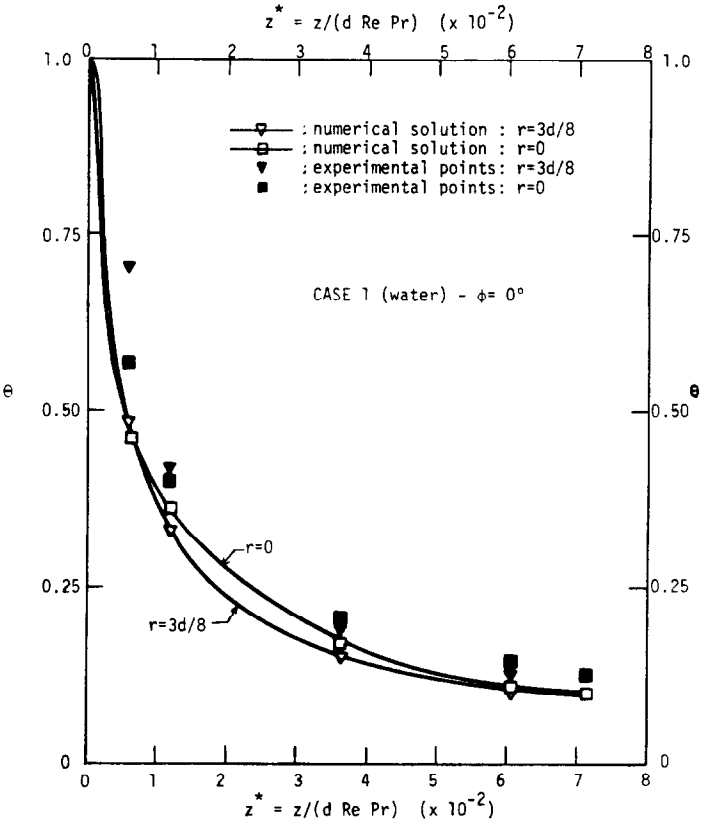

FIG. 5. Dimensionless temperature axial variation.

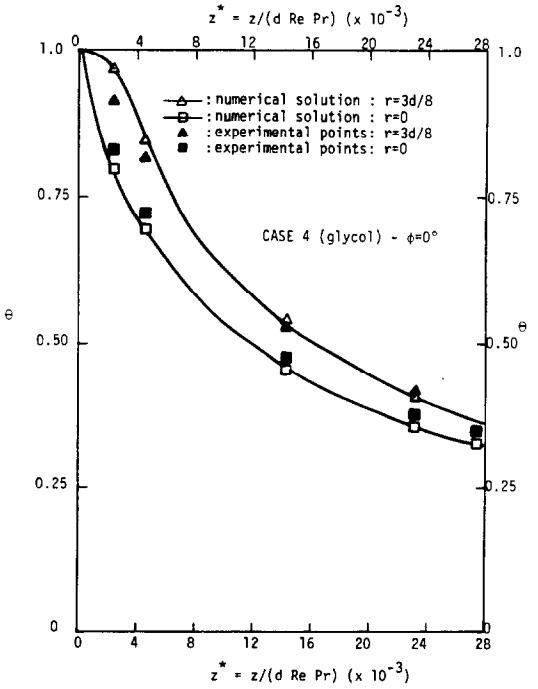

FIG. 6. Dimensionless temperature axial variation.

water are below the experimental data (cf. Fig. 5), while, for glycol (cf. Fig. 6), the calculated values are above at $r = 3d/8$ and below at $r = 0$.

Figure 7 shows the radial variation of the temperature at various axial locations at $\phi = 0°$. The variation of the temperature is similar to that found for the isothermal wall condition [22], with the exception that the profile between the maximum (occurring near $r = 5d/12$) and the tube axis is non-monotonic for the present boundary condition. This effect will be discussed in conjunction with the streamline patterns. However, the strong secondary flows still create a temperature profile which reaches a maximum at a radial location close to the center of the streamline patterns (maximum value of the stream function).

Figure 8 presents the wall temperature variation with respect to the angle ϕ at several axial locations. The large variation in the wall temperature (about 10°C near the entrance) experienced in case 3 (Fig. 8) indicates that this boundary condition creates a flow pattern and a heat transfer process which varies strongly with respect to the angle ϕ. The calculations are in good agreement with the experimental data, especially over the second half of the tube length.

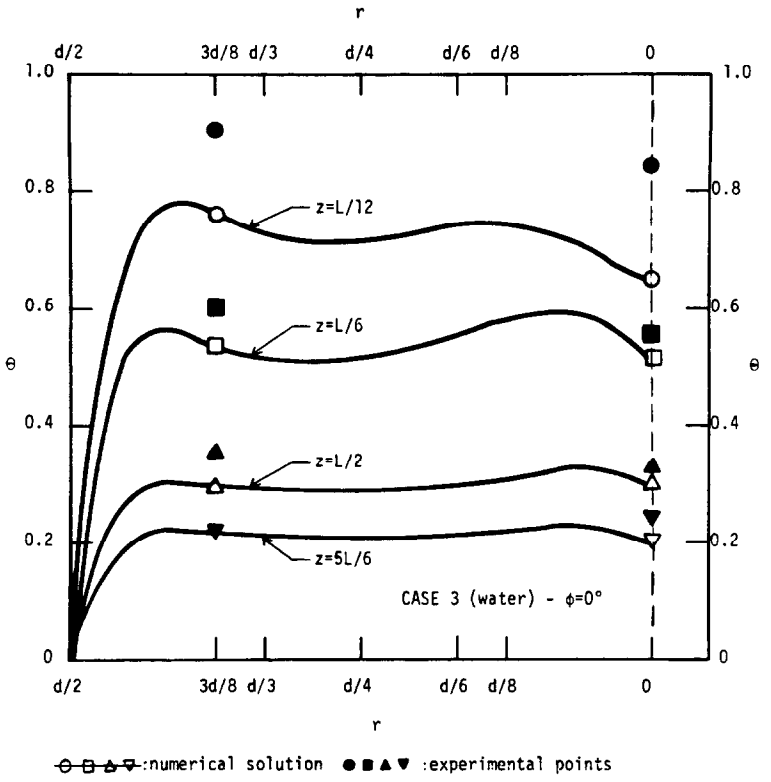

FIG. 7. Dimensionless temperature radial variation.

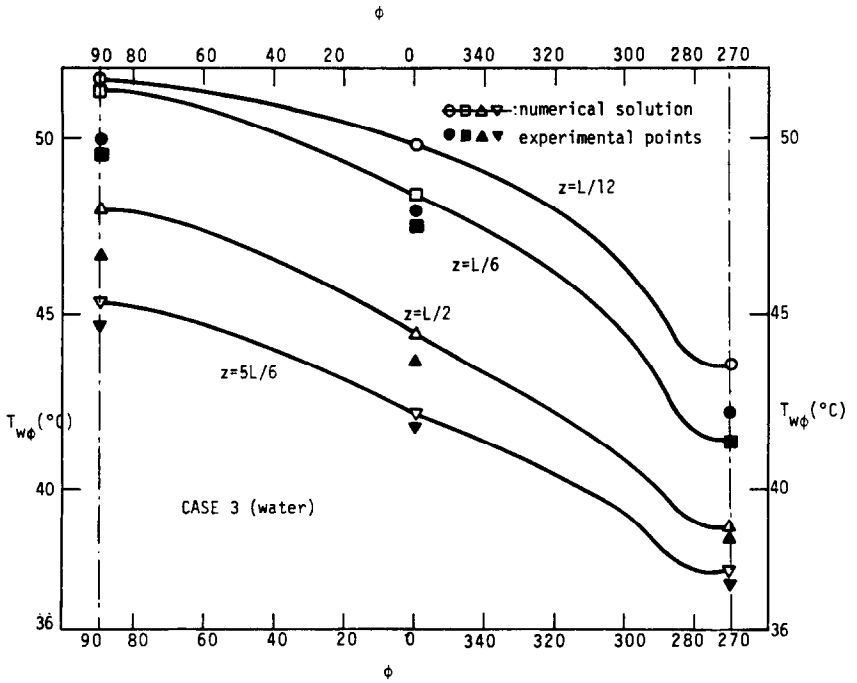

FIG. 8. Dimensionless temperature radial variation.

B. Calculated heat transfer results

Figure 9 shows the axial variation of the calculated local inside Nusselt number at various angles. Also plotted is the average Nusselt number (calculated by averaging the local values over the full range of angles ϕ). For the entrance region, the non-monotonic behavior of the Nusselt number is due to the developing secondary flow which reaches the top of the tube after the axial motion has carried the fluid to the location $z = L/10$ [22]. The difference in the Nusselt numbers between the curves for $\phi = 80°$ and $0°$ and between $\phi = 0°$ and $280°$ is larger than for the isothermal wall condition. This is attributed to the stronger angular dependence of the secondary flow effect, which is now considered.

Figure 10 presents the angular variation of the local Nusselt number at four axial locations. The decrease after $\phi = 0°$ shows that most of the energy from the fluid has been transferred over the upper portion of the tube. The Nusselt number profile is essentially a constant in the upper part of the tube, for all axial locations. This was not true for the constant wall temperature condition [22, 23]. Under the isothermal wall condition [22], only the bulk fluid temperature decreased with ϕ, whereas, in the present condition, both the fluid and the wall temperatures decrease. It is noted that the local Nusselt numbers at $\phi = 280°$ do not show a strong axial dependence.

C. Other theoretical predictions

In Figs. 11 and 12, the streamlines are plotted on the left side of the figure and the isotherms on the right side. Figure 11 presents a comparison of the two boundary conditions for two cases with comparable values of the characteristic quantity Gr/Re^2. Both cross-sectional variations are shown for the axial location $z = L/12$. For the case of natural convection around the boundary, one observes that the fluid flows down along the walls and continues down to nearly the bottom of the tube. This is due to the continuous temperature decrease along the wall (cf. Fig. 8), resulting in a sustained cooling of the fluid as it moves down near the

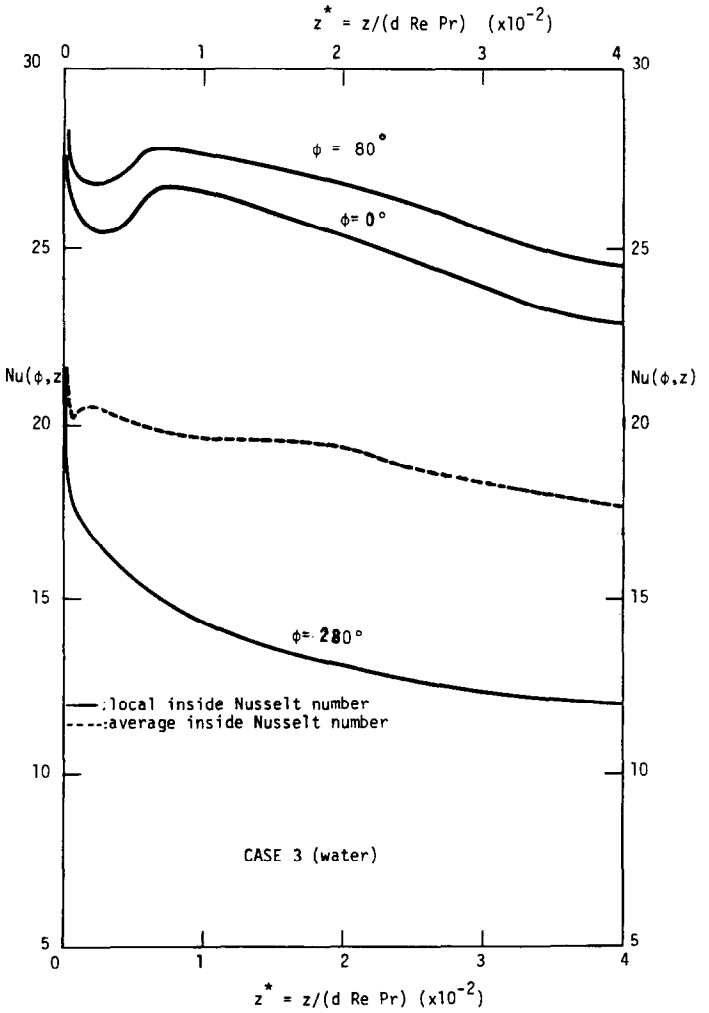

FIG. 9. Local and average Nusselt number axial variation.

wall. For the constant wall temperature condition, the fluid was more strongly cooled in the upper part of the tube [22, 23] and therefore, the buoyancy force decreased rapidly as the fluid moved down. As an example, the magnitude of the secondary velocity at point O is five times larger for the top picture (natural convection) than for the bottom picture (isothermal wall). Clearly, the secondary flows in the isothermal wall case have less momentum at this location. For the natural convection boundary condition, the fluid continues downward and only rises near the bottom of the tube. The fluid moves up near the vertical diameter until it reaches a location below the center (point A). The buoyant vertical forces are not strong, (cf. the isotherms on the right side of the graph). Since the fluid cannot cross the vertical plane, it turns away from the center and is heated as illustrated by the temperature gradient between points A′ (symmetrical with A about the vertical diameter) and B′. Thus the motion in that region is clockwise as shown by the streamlines on Fig. 11. There is also a small recirculation near the center of the tube.

This phenomenon is a clear example of a situation where the overall fluid motion is strongly affected by the boundary condition. The secondary flow patterns described above were found, numerically for all five cases studied, to be independent of the operating conditions and the fluid type. Figure 12 represents the secondary flow patterns at an axial location $z = 5L/6$ which demonstrates that, even far down the tube, the preceding observations remain true. No significant change in the size of the bean-shaped streamlines was found numerically when comparing all cases for different values of the characteristic quantity Gr/Re^2.

CONCLUSIONS

When a horizontal tube is subjected to mixed laminar convection on the inside and natural convection on the outside, the internal fluid flow is very complex. Even when the study of the outer fluid movement is simplified by the introduction of an empirical correlation, the three-dimensional flow inside the tube remains very difficult to analyze. The present study underlines the importance of secondary

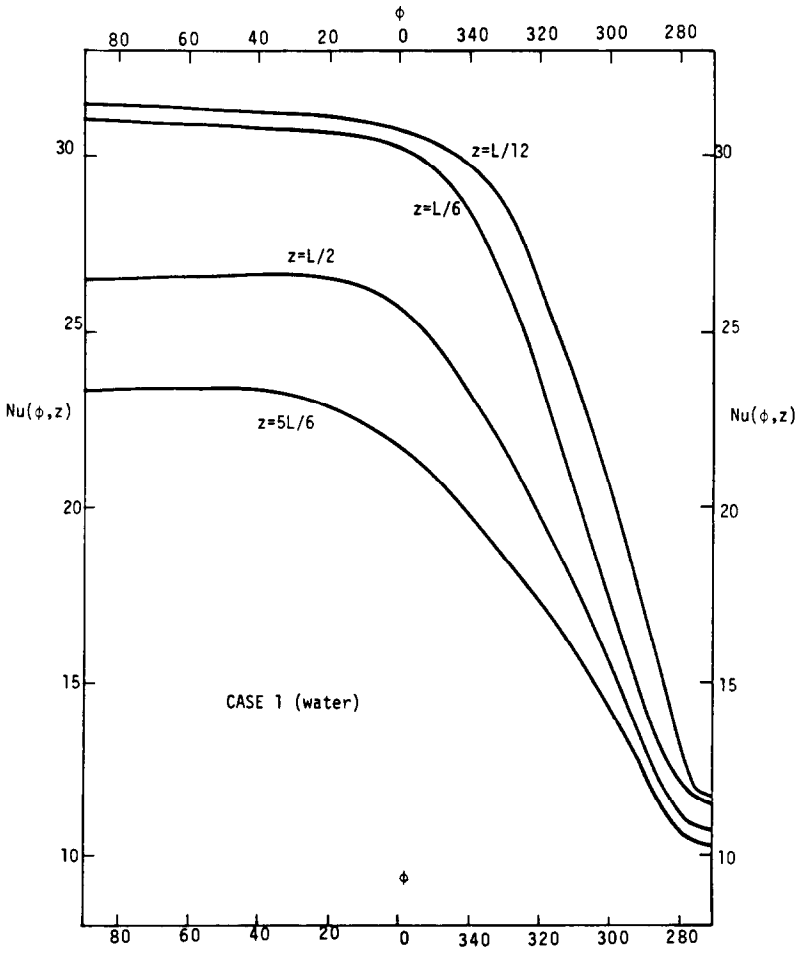

FIG. 10. Local Nusselt number angular variation.

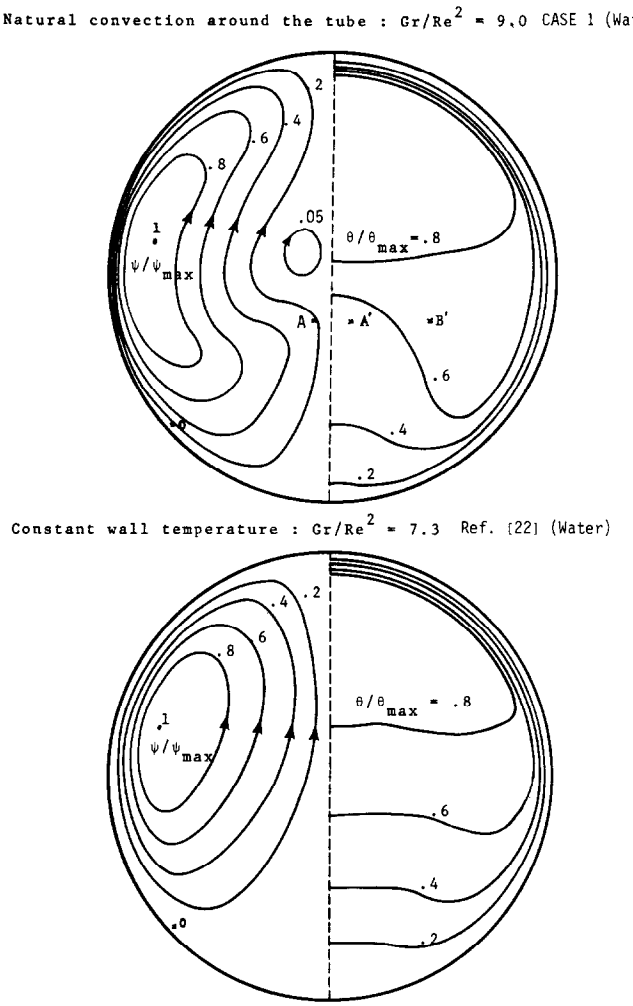

FIG. 11. Comparison of streamlines and isotherms at $z = L/12$.

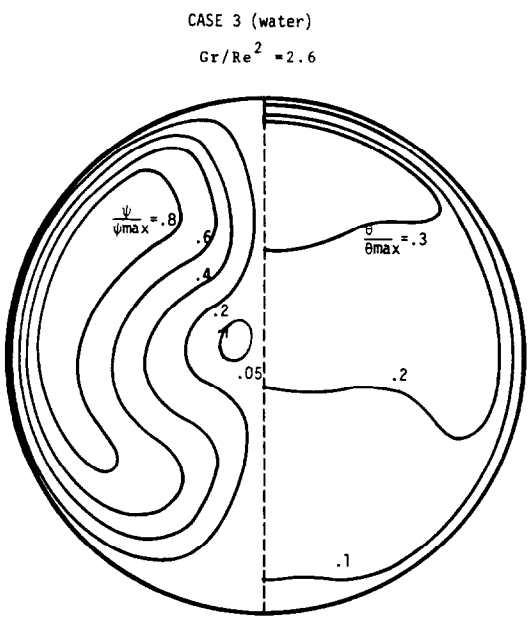

FIG. 12. Streamlines and isotherms at $z = 5L/6$.

flows within the tube and demonstrates their effect on the heat transfer.

When the outer surface of the tube wall is subjected to natural convection, the wall temperature exhibits large angular differences. In addition, the wall temperature varies axially, since the surrounding fluid is not replaced in the storage tank. This highly variable boundary temperature complicates even further the phenomena previously observed in the related problem of isothermal wall conditions. In particular, the numerical study led to the prediction of bean-shaped secondary flow patterns. Significant differences were found for the cross-sectional flow patterns when comparing the two boundary conditions. The strong angular dependence of the phenomena described suggests the need for three-dimensional calculations to determine the heat transfer in many developing tube flows.

REFERENCES

1. T. H. Kuehn and J. L. Balvanz, Conjugate heat transfer by natural convection from a horizontal heat exchanger tube. *Proc. Heat Transfer Conference*, Munich, pp. NC33 : 317–322 (August 1982).
2. B. Sunden, Conjugated heat transfer from circular cylinders in low Reynolds number flow, *Int. J. Heat Mass Transfer* **23**, 1359–1367 (1980).
3. M. Faghri and E. M. Sparrow, Forced convection in a horizontal pipe subjected to nonlinear external natural convection and to external radiation, *Int. J. Heat Mass Transfer* **24**, 861–872 (1981).
4. A. M. Abdelmeguil and D. B. Spalding, Turbulent flow and heat transfer in pipes with buoyancy effects, *J. Fluid Mech.* **94**, 383–400 (1979).
5. V. Javeri, Simultaneous development of the laminar velocity and temperature fields in a circular duct for the temperature boundary condition of the third kind, *Int. J. Heat Mass Transfer* **19**, 943–949 (1976).
6. S. Golos, Theoretical investigation of the thermal entrance region in steady, axially symmetrical slug flow with mixed boundary conditions, *Int. J. Heat Mass Transfer* **13**, 1715–1725 (1970).
7. T, H. Kuehn and R. J. Goldstein, Numerical solution to the Navier–Stokes equations for laminar natural convection about a horizontal isothermal circular cylinder, *Int. J. Heat Mass Transfer* **23**, 971–979 (1980).
8. T. H. Kuehn and R. J. Goldstein, Correlating equations for natural convection heat transfer between horizontal circular cylinders, *Int. J. Heat Mass Transfer* **19**, 1127–1134 (1976).
9. S. W. Churchill and R. Usagi, A general expression for the correlation of rates of transfer and other phenomena, *Am. Inst. chem. Engrs J.* **18**, 1121–1128 (1972).
10. J. A. Peterka and P. D. Richardson, Natural convection from a horizontal cylinder at moderate Grashof numbers, *Int. J. Heat Mass Transfer* **12**, 749–752 (1969).
11. A. Mojtabi and J. P. Caltagirone, Analyse du transfert de chaleur en convection mixte laminaire entre deux cylindres coaxiaux horizontaux, *Int. J. Heat Mass Transfer* **23**, 1369–1375 (1980).
12. F. N. Lin and B. T. Chao, Laminar free convection over two-dimensional and axisymmetric bodies of arbitrary contour, *Trans. Am. Soc. mech. Engrs*, Series C, *J. Heat Transfer* **96**, 435–442 (1974).
13. T. Aihara and E. Saito, Measurement of free convection velocity field around the periphery of a horizontal torus, *Trans. Am. Soc. mech. Engrs*, Series C, *J. Heat Transfer* **94**, 95–98 (1972).
14. A. Acrivos, Combined laminar free and forced convection heat transfer in external flows, *Am. Inst. chem. Engrs J.* **4**, 285–289 (1958).
15. W. N. Gill and A. J. Bardhun, Experiments in horizontal tubes including observations on natural convection effects, *Am. Inst. chem. Engrs J.* **12**, 916–921 (1966).
16. S. W. Churchill and H. H. S. Hsu, Correlating equations for laminar and turbulent free convection from a horizontal cylinder, *Int. J. Heat Mass Transfer* **18**, 1049–1053 (1975).
17. V. T. Morgan, The overall convective heat transfer from smooth circular cylinders, *Adv. Heat Transfer* **11**, 199–264 (1975).
18. A. D. Gosman and F. J. K. Ideriah, TEACH-2E: A general computer program for two dimensional, turbulent, recirculating flows, Imperial College, London, and University of California (1983).
19. J. A. C. Humphrey, Numerical calculation of developing laminar flow in pipes of arbitrary curvature radius, *Can. J. chem. Engng* **56**, 151–164 (1978).
20. S. V. Patankar, *Numerical Heat Transfer and Fluid Flow*. McGraw-Hill, New York (1980).
21. A. Lavine, A three-dimensional numerical analysis of fluid flow and heat transfer in a toroidal thermosyphon. Master's thesis, University of California (March 1983).
22. P. Coutier and R. Greif, An investigation of laminar mixed convection inside a horizontal tube with isothermal wall conditions, *Int. J. Heat Mass Transfer*, **28**, 1293–1306 (1985).
23. P. Coutier, Laminar convection with buoyancy in tube flows with a Surrounding liquid medium. Ph.D. thesis, University of California, Berkeley (1983).

CONVECTION LAMINAIRE MIXTE DANS UN TUBE HORIZONTAL AVEC CONVECTION NATURELLE SUR LA FRONTIERE EXTERNE

Résumé—On étudie à la fois expérimentalement et numériquement l'écoulement laminaire et le transfert thermique dans un tube horizontal entouré par un liquide. On porte l'attention sur les régimes d'écoulement ou un effet d'Archimède s'ajoute à l'écoulement forcé dans le tube. La surface externe du tube est soumise à la convection naturelle résultant de la différence de température entre la paroi et le fluide environnant. Des analyses détaillées sont conduites pour un groupe de cas avec différents fluides, température d'entrée et débits. On montre que la température variable de la paroi a un effet marqué sur la configuration de l'écoulement secondaire dans le tube aussi bien que le transfert de chaleur.

GEMISCHTE LAMINARE KONVEKTION IN EINEM HORIZONTALEN ROHR MIT NATÜRLICHER KONVEKTION AN DEN GRENZFLÄCHEN

Zusammenfassung—Es wird die Laminarströmung und der Wärmeübergang in einem waagerechten Rohr, das von einem flüssigen Medium umgeben ist, experimentell und numerisch untersucht. Besondere Beachtung finden die Bereiche, in denen sich Auftriebseffekte bei der erzwungenen Strömung im Rohr zeigen. An der Außenoberfläche des Rohres stellt sich ebenfalls natürliche Konvektion ein, die aufgrund der Temperaturdifferenz zwischen Wand und umgebendem Fluid entsteht. Für eine Reihe von Beispielen mit verschiedenen Fluiden, Eintrittstemperaturen und Strömungsgeschwindigkeiten werden detaillierte Analysen durchgeführt. Dabei stellt sich heraus, daß die Wandtemperatur einen großen Einfluß auf die Formen der Sekundärströmung im Rohr und auf den Wärmeübergang hat.

СМЕШАННАЯ ЛАМИНАРНАЯ КОНВЕКЦИЯ В ГОРИЗОНТАЛЬНОЙ ТРУБЕ СО СВОБОДНОЙ КОНВЕКЦИИ У ЕЕ ВНЕШНЕЙ ПОВЕРХНОСТИ

Аннотация—Численно и экспериментально изучаются ламинарное течение и теплоперенос внутри горизонтальной трубы, находящейся в жидкости. Основное внимание уделяется режимам течения в трубе, для которых существенным является влияние подъемной силы. На внешнюю поверхность трубы воздействуют свободная конвекция, возникающая из-за разности температур между стенкой и окружающей жидкостью. Детально анализируются случаи для различных жидкостей и их расходов, температур на входе и выходе. Установлено, что переменная температура стенки оказывает значительное влияние на характеристики вторичных течений внутри трубы, а также на теплоперенос.